CANCER BIOTHERAPY & RADIOPHARMACEUTICALS
Volume 16, Number 1, 2001
Mary Ann Liebert, Inc.

In Vivo and In Vitro Measurement of Apoptosis in Breast Cancer Cells Using ^{99m}Tc-EC-Annexin V

David J. Yang, Ali Azhdarinia, Peng Wu, Dong-Fang Yu, Wayne Tansey, Saady Kohanim Kalimi, E. Edmund Kim, and Donald A. Podoloff
Department of Nuclear Medicine, The University of Texas M. D. Anderson Cancer Center, Houston, Texas

Objective: *The purpose of this study was to develop an imaging technique to measure and monitor tumor cells undergoing programmed death caused by radiation and chemotherapy using ^{99m}Tc-EC-annexin V. Annexin V has been used to measure programmed cell death both in vitro and in vivo. Assessment of apoptosis would be useful to evaluate the efficacy and mechanisms of therapy and disease progression or regression.* ***Methods:*** *Ethylenedicysteine (EC) was conjugated to annexin V using sulfo-N-hydroxysuccinimide and 1-ethyl-3-(3-dimethylaminopropyl) carbodiimide-HCl as coupling agents. The yield of EC-annexin V was 100%. In vitro cellular uptake, pre- and post-radiation (10–30 Gy) and paclitaxel treatment, was quantified using ^{99m}Tc-EC-annexin V. Tissue distribution and planar imaging of ^{99m}Tc-EC-annexin V were determined in breast tumor-bearing rats at 0.5, 2, and 4 hrs. To demonstrate in vivo cell apoptosis that occurred during chemotherapy, a group of rats was treated with paclitaxel and planar imaging studies were conducted at 0.5–4 hrs. Computer outlined region of interest (ROI) was used to quantify tumor uptake on day 3 and day 5 post-treatment.* ***Results:*** *In vitro cellular uptake showed that there was significantly increased uptake of ^{99m}Tc-EC-annexin V after irradiation (10–30 Gy) and paclitaxel treatment. In vivo biodistribution of ^{99m}Tc-EC-annexin in breast tumor-bearing rats showed increased tumor-to-blood, tumor-to-lung and tumor-to-muscle count density ratios as a function of time. Conversely, tumor-to-blood count density ratios showed a time-dependent decrease with ^{99m}Tc-EC in the same time period. Planar images confirmed that the tumors could be visualized clearly with ^{99m}Tc-EC-annexin. There was a significant difference of ROI ratios between pre- and post-paclitaxel treatment groups at 2 and 4 hrs post injection.* ***Conclusion:*** *The results indicate that apoptosis can be quantified using ^{99m}Tc-EC-annexin and that it is feasible to use ^{99m}Tc-EC-annexin to image tumor apoptosis.*

Key words: Apoptosis, ^{99m}Tc-EC-annexin

INTRODUCTION

Breast cancer is the second leading cause of death among women with cancer. Early prediction of the likelihood of treatment response can lead to more effective treatment and reduced mortality. Currently, assessment of breast cancer treatment response relies on tumor markers, e.g., CA125, tissue biopsy or imaging.[1–6] However, tumor markers are influenced by other factors, so that they lack sensitivity and specificity, while tissue biopsy is an invasive process associated with sampling errors.

Conventional x-ray mammography has been shown to reduce mortality of breast cancer by about 30% in women older than 50 years of age and by 17% in women ages 40–50.[7,8] Though mammography is relatively inexpensive, it is not

Address reprint requests to David J. Yang, PhD, Univ. of Texas M. D. Anderson Cancer Center, Dept. of Nuclear Medicine, Box 59, 1515 Holcombe Boulevard, Houston, Texas 77030 Tel: (713) 794-1053 Fax: (713) 794-5456 E-mail: dyang@di.mdacc.tmc.edu

sensitive in detecting breast cancer (25–30%) in women with dense breast tissue,[7] and is not useful for early prediction of therapeutic response. Similarly, computed tomography (CT), ultrasound, and chest x-rays are not helpful in predicting therapeutic response. MRI is used to follow-up on treatment changes, providing perfusion and diffusion information, with the status of blood flow.[9] Molecular targets (e.g., estrogen, progestin, folate, retinoic acid receptors, BRCA-1, HER-2/neu, p53, cyclin D1) provide more accurate functional information for breast cancer diagnosis and treatment.[10–17] Tagging molecular targets with radionuclides can increase our understanding of pharmacokinetic, pharmacodynamic and metabolic imaging patterns of the agent, thereby providing information useful for characterizing tumors.

Apoptosis, programmed cell death, is a natural, orderly, energy-dependent process that causes cells to die without inducing an inflammatory response.[18,19] Apoptosis is triggered either by a decrease in factors required to maintain the cell in good health or by an increase in factors that cause damage to the cell.[20,21] When these factors tilt in the direction of death and the cell has sufficient time to respond, a proteolytic cascade involving cysteine aspartic acid-specific proteases (caspases) is activated to initiate apoptosis.[22]

Cells that die by apoptosis autodigest their DNA and nuclear proteins, change the phospholipid composition on the outer surface of their cell membrane, and form lipid enclosed vesicles, which contain noxious intracellular contents, organelles, autodigested cytoplasm, and DNA. The compositional cell membrane phospholipid change that occurs with the onset of apoptosis is marked by the expression of phosphatidylserine (PS). PS, a phospholipid that constitutes 10–15% of phospholipid content and appears on the inner leaflet of the membrane, is redistributed onto the external leaflet of the membrane during apoptosis.[23]

Annexin V binds to phosphatidylserine during apoptosis,[24–26] and radiolabeled annexin V may be useful in evaluating the efficacy of therapy and disease progression or regression. Imaging of apoptosis has been achieved by ultrasound,[27] confocal laser scanning microscopy[28] and a fluorescent probe.[29] Fluorescence-labeled annexin V is used for histologic and cell-sorting studies to identify apoptotic cells. Due to the sensitivity, specificity, accessibility, and cost, this technique is not suitable for in vivo imaging studies. ^{99m}Tc-HYNIC-annexin has been shown to be useful in imaging apoptosis in liver transplantation in animal models.[30–32] However, labeling HYNIC with ^{99m}Tc requires two other chemicals, thiphenylphosphine and tricin, which are inconvenient for the formation of a kit preparation. Among all chelators for ^{99m}Tc- chemistry, L,L-ethylenedicysteine (EC) is the most stable and successful example of N_2S_2 chelates.[33–40] EC-drug conjugates can be labeled with ^{99m}Tc easily and efficiently with high radiochemical purity and stability. Thus, we developed a noninvasive method to detect and measure apoptosis by tagging annexin with ^{99m}Tc- using EC as a chelator. In this paper, synthesis, cellular uptake, biodistribution, breast tumor imaging, and quantification of treatment changes using ^{99m}Tc-EC-annexin V are reported.

MATERIALS AND METHODS

Synthesis of L,L-Ethylenedicysteine (EC)

Mass spectral analyses were conducted at the University of Texas Health Science Center (Houston, TX). Nuclear magnetic resonance (NMR) spectra were recorded on a Bruker-300 Spectrometer. The mass data were obtained by fast atom bombardment on a Kratos MS 50 instrument (England). N-hydroxysulfosuccinimide (Sulfo-NHS) and 1-ethyl-3-(3-dimethylaminopropyl) carbo-diimide-HCl (EDC) were purchased from Pierce Chemical Co (Radford, IL). All other chemicals were purchased from Aldrich Chemical Co (Milwaukee, WI). Silica gel coated thin-layer chromatography (TLC) plate was purchased from Whatman (Clifton, NJ). EC was prepared in a two-step synthesis according to the previously described methods.[41,42] The precursor, L-thiazolidine-4-carboxylic acid, was synthesized (m.p. 195°, reported 196–197°). EC was then prepared (m.p. 243°C, reported 251°C).

Synthesis and Radiolabeling of EC-Annexin

Sodium bicarbonate (1N, 1 ml) was added to a stirred solution of EC (5 mg, 0.019 mmol). To this colorless solution, sulfo-NHS (4 mg, 0.019 mmol) and EDC (4 mg, 0.019 mmol) were added. Annexin V (M.W. 33 kD, human, Sigma Chemical Company) (0.3 mg) was then added. The mixture was stirred at room temperature for 24 hrs. The mixture was dialyzed for 48 hrs with cut-off at M.W.10,000. After dialysis, the product was freeze dried, with the product in the salt form weighing 0.5 mg.

^{99m}Tc-pertechnetate was obtained from Syncor Pharmaceutical Inc. (Houston, TX). Radiosynthesis of ^{99m}Tc- EC-annexin was achieved by adding the required amount of ^{99m}Tc-pertechnetate into EC-annexin (50 μg) and tin chloride (II) ($SnCl_2$, 100 μg). The mixture was loaded on a sephadex gel column (PD-10, G-25, Pharmacia Biotech, Swiss) and eluted with phosphate buffered saline (pH 7.4). One ml of each fraction was collected. The product was collected at fraction 3, yielding 70%. Radiochemical purity was assessed by Radio-TLC (Bioscan, Washington, DC) using 1M ammonium acetate: methanol (4/1) as an eluant and HPLC. HPLC, equipped with NaI detector and UV detector (254 nm), was performed on a GPC column (Biosep SEC-S3000, 7.8 $\times$ 300 mm, Phenomenex, Torrance, CA) using a flow rate of 1.0 ml/min. The eluant was 0.1% LiBr in PBS (10 mM, pH = 7.4).

In Vitro Cellular Uptake Assay

Paclitaxel-induced apoptosis

Breast tumor cells were obtained from RBA CRL-1747 rat breast cancer cell line (American Type Culture Collection, ATCC, Rockville, MD). This cell line was derived from a tumor induced in Fischer-344 rat by giving an oral dose of 7,12-dimethyl-benz[a]anthracene. The cells were cultured in Eagle's MEM with Earle's BSS (90%) and fetal bovine serum (10%). Breast tumor cells (5.0×10^4 cells/0.5 ml buffer/well) were treated with paclitaxel (0–100 ng/20 μl/well). After 24 hrs incubation, cell viability was determined by methylene tetrazolium (MTT) assay.[43] ^{99m}Tc-EC-annexin (2 μCi/well, 1.5 μg/well) was added to the cells. After 2 and 4 hrs incubation, the cells were washed twice with ice cold PBS (1 ml), and trypsin EDTA (0.1 ml) was added. After 2 min, PBS (0.4 ml) was added and the total volume containing cells was transferred to a test tube to count the activity. ^{99m}Tc-pertechnetate was used as a control. Each data represents an average of four measurements, that were calculated as percentage of uptake per number of viable cells.

Radiation-induced apoptosis

To quantify cellular uptake during the apoptotic process using ^{99m}Tc-EC-annexin V, breast tumor cells (2.5×10^5 cell/5 ml buffer/well) were irradiated with a Cs-137 external beam source (0–30 Gy/well). After three-day incubation, cell viability was determined by MTT assay. ^{99m}Tc-EC-annexin (10 μCi/well, 7.5ìg/well) was added to the cells. After 2 hrs incubation, the cells were washed twice with ice cold PBS (1 ml), after which trypsin EDTA (0.5 ml) was added. After 2 min, PBS (2 ml) was added. Unbound ^{99m}Tc-EC-annexin was removed by centrifugation and the total volume containing the cells was transferred to a test tube to count the activity. Each data represents an average of three measurements, that were calculated as percentage of uptake per number of viable cells.

Apoptotic cells were simultaneously quantified by fluorescence microscopic enumeration of apoptotic cells using Hoechst 33342 staining (Fisher Scientific, Houston, TX). The Hoechst 33342 morphological analysis was chosen as a nondestructive method in which the classic morphology of early, late apoptotic cells and early membrane permeability changes can be evaluated on intact cells.[44] Briefly, fresh cells were stained with Hoechst 33342 at 0.1 μg/ml in complete medium for 15 min at 37°C. Cell morphology was examined using an inverted fluorescence microscope (Wetzlar, Leica, Germany).

Tissue Distribution Studies

Female Fischer 344 rats (150–25 g) (Harlan Sprague-Dawley, Indianapolis, IN) were inoculated subcutaneously with 0.1 ml of mammary tumor cells from the RBA CRL-1747 rat breast cancer cell line (10^6 cells/rat) into the hind legs. Studies were performed 14 to 17 days after implantation when tumors reached approximately 1 cm in diameter.

In tissue distribution studies, each animal was injected intravenously (i.v.) with ^{99m}Tc- EC-annexin or ^{99m}Tc-EC (10 μCi/rat, n = 3 rats/time point) through tail vein. The injected mass of each ligand was 10 μg per rat. At 30 min, 2 and 4 hrs following administration of the radiotracers, the animals were sacrificed and the tumor and selected tissues were excised, weighed and counted for radioactivity by using a gamma counter (Packard Instruments, Downers Grove, IL). The biodistribution of tracer in each sample was calculated as percentage of the injected dose per gram of tissue wet weight (%ID/g). Student-t test was used to assess the significance of differences between two groups.

Scintigraphic Imaging Studies

Scintigraphic images, using a gamma camera (Siemens Medical Systems, Inc., Hoffman Es-

tates, IL) equipped with low-energy parallel-hole collimator were obtained 0.5–4 hrs after intravenous injection of 100 μCi ^{99m}Tc-EC-annexin. To ascertain the tumor treatment response, the same pre-imaged rats were administered paclitaxel (40 mg/kg, iv tail vein, day 14) and images were taken on days 16 and 18. Computer outlined regions of interest (ROI) (counts per pixel) were used to determine tumor-to-background count density ratios. The ratios were used to compare dynamic tumor uptake pre- and post-treatment. Errors in the use of image ROIs as standards to correspond to anatomically relevant features have been described and found tolerable.[45,46]

RESULTS

Chemistry

EC was conjugated to amino or lysine residue of annexin V. A simple and efficient synthesis of ^{99m}Tc-EC-annexin was developed. ^{99m}Tc-EC-annexin was found to be radiochemically pure (100%). The retention time of ^{99m}Tc-EC-annexin was at 9.63 min (Figure 1). Under the same condition, the retention time of ^{99m}Tc-EC (control) was at 14.03 min (data not shown). The amount injected to HPLC was 3 μCi per 22.5 ng of ^{99m}Tc-EC-annexin. The specific activity was calculated to be 5 Ci/μmol.

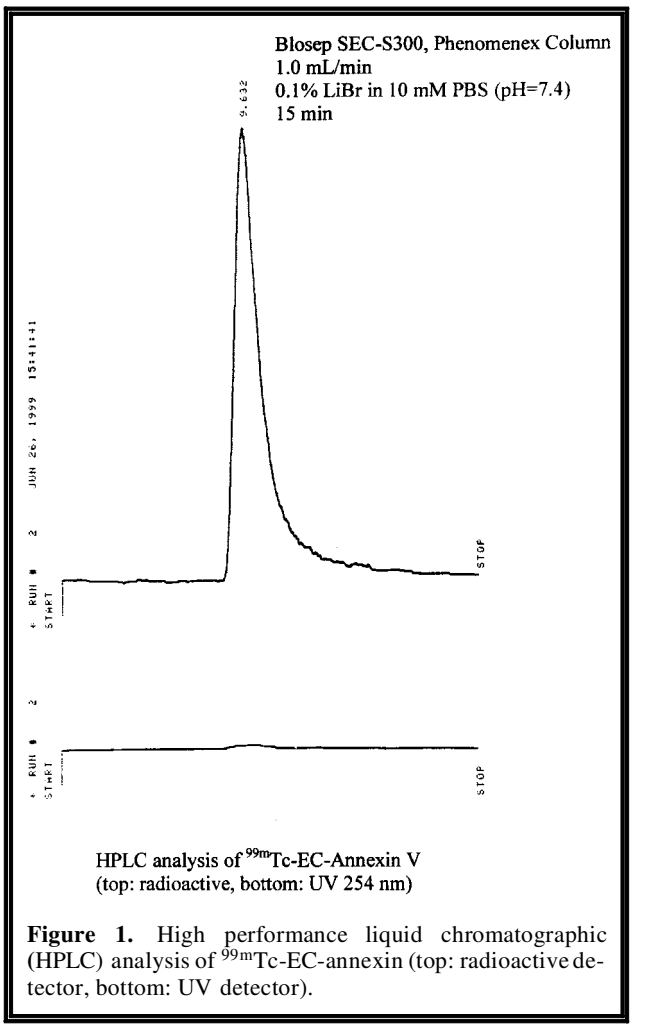

Figure 1. High performance liquid chromatographic (HPLC) analysis of ^{99m}Tc-EC-annexin (top: radioactive detector, bottom: UV detector).

In Vitro Cellular Uptake Assay

Paclitaxel-induced apoptosis

There was a markedly increased uptake of ^{99m}Tc-EC-annexin V in the paclitaxel (100 ng/well) treated group compared to non-treated groups at 2 and 4 hours incubation (Figure 2). Similar findings in the paclitaxel (50 ng/well) treated group at 4 hours incubation were observed. This increased uptake is likely due to apoptotic bodies formed in the cells which correlates with the appearance of apoptotic bodies shown in Figures 3 and 4. Apoptotic cells were brightly stained and the classic progression of chromatin condensation and nuclear fragmentation was visible. The in vitro findings indicated that ^{99m}Tc-EC-annexin V is useful in measuring apoptotic processes before and after paclitaxel treatment.

Radiation-induced apoptosis

Significantly increased uptake of ^{99m}Tc-EC-annexin V was observed in radiation-treated groups (10 and 30 Gy) compared to non-treated groups at 2 hours incubation (Figure 5).

In Vivo Biodistribution and Scintigraphic Imaging Studies

In biodistribution studies, unlike ^{99m}Tc-EC groups (Table 1), tumor-to-tissue count density ratios in ^{99m}Tc-EC-annexin groups showed an increased uptake as a function of time (Table 2). Tumor uptake (%ID/G) in ^{99m}Tc-EC-annexin groups was higher than ^{99m}Tc-EC. Liver uptake in ^{99m}Tc-EC-annexin groups was also higher than ^{99m}Tc-EC groups. The difference in liver uptake may be due to their different molecular weights (M.W. 35,000 of annexin vs 268 of EC). Although high uptake in kidneys was observed in ^{99m}Tc-EC and ^{99m}Tc-EC-annexin groups, this may be due to the route of excretion of both agents.

Scintigraphic images of ^{99m}Tc-EC-annexin

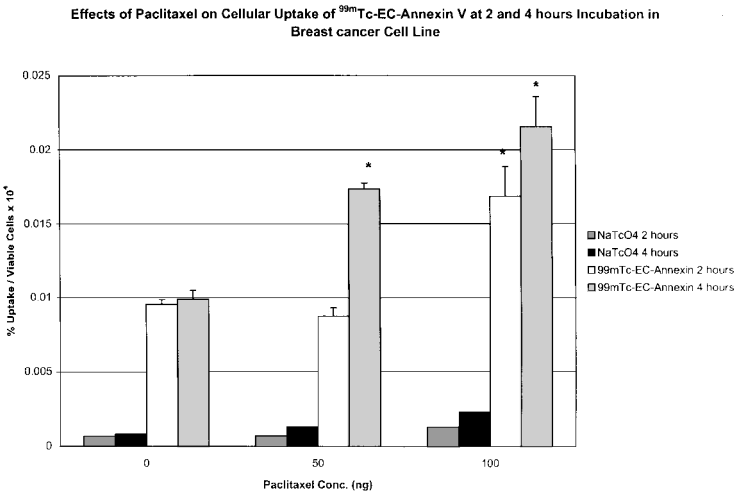

Figure 2. Breast cancer cell line (RBA CRL-1747, 5.0×10^4 cells/well) was selected for this study. Cell culture was performed in 24-well plate. After adding paclitaxel (0–100 ng/well), followed by 24 hrs incubation, ^{99m}Tc-EC-annexin V (2μCi) was added to each well and incubated for 2–4 hours. Each bar represents an average of four measurements. Viable cells were determined by methylene tetrazolium (MTT) assay. Each data was calculated as percentage of uptake per number of viable cells. There was a markedly increased uptake of ^{99m}Tc-EC-annexin V in paclitaxel treated groups (50 and 100 ng) compared to non-treated groups at 4 hrs incubation. An asterisk indicates significant ($p < 0.05$) difference between treated and untreated groups at the same time interval.

demonstrated that these relatively large tumors could be visualized well on day 14 after inoculation of tumor cells (Figure 6). However, there was a significantly increased uptake (ROI ratios) of ^{99m}Tc-EC-annexin in tumors after paclitaxel treatment when compared to pretreatment uptake. Differences were observed in ROI ratios between pre- and post-treatment on day 5 post-treatment at 2 hrs and on day 3 post-treatment at 1, 2 and 4 hrs (Table 3).

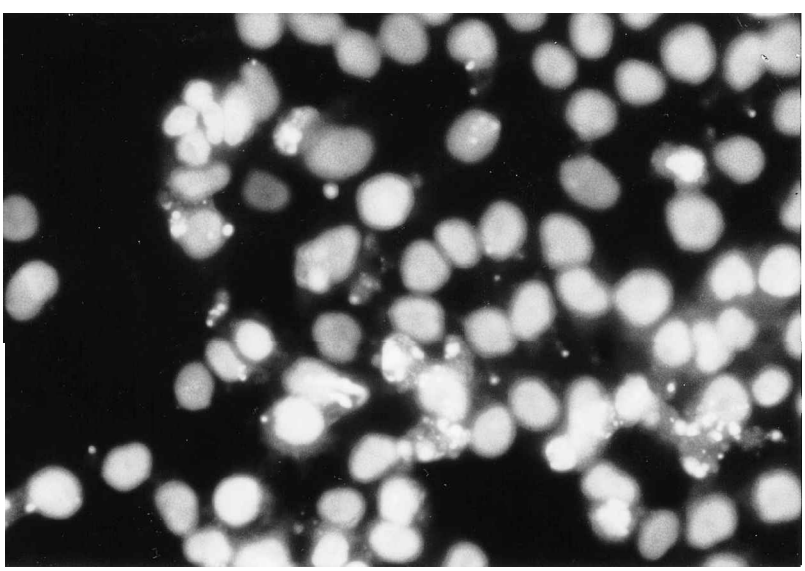

Figure 3. Fresh cells were stained with Hoechst 33342 at 0.1 μg/ml in complete medium for 15 min at 37°C. Cell morphology was examined using an inverted fluorescence microscope (40×). The cells showed clear cell body and cell nuclei prior to paclitaxel treatment.

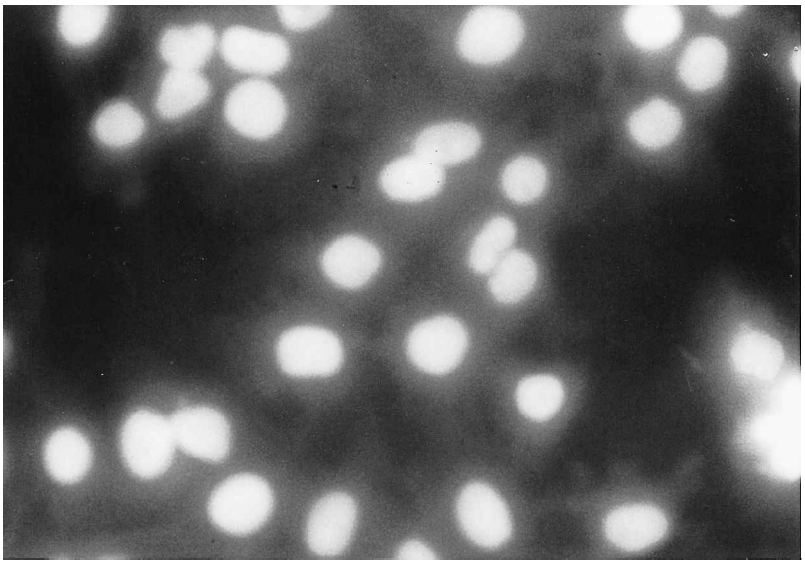

Figure 4. Apoptotic cells were simultaneously quantified by fluorescence microscopic enumeration of apoptotic cells using Hoechst 33342 staining. Formation of apoptotic bodies were present in cells post-paclitaxel treatment.

DISCUSSION

Improvement of scintigraphic tumor diagnosis, prognosis, planning, and monitoring of treatment of cancer will clearly be determined by the development of more tumor-specific radiopharmaceuticals. Radionuclide imaging modalities (positron emission tomography, PET; single photon emission computed tomography, SPECT) are diagnostic cross-sectional imaging techniques

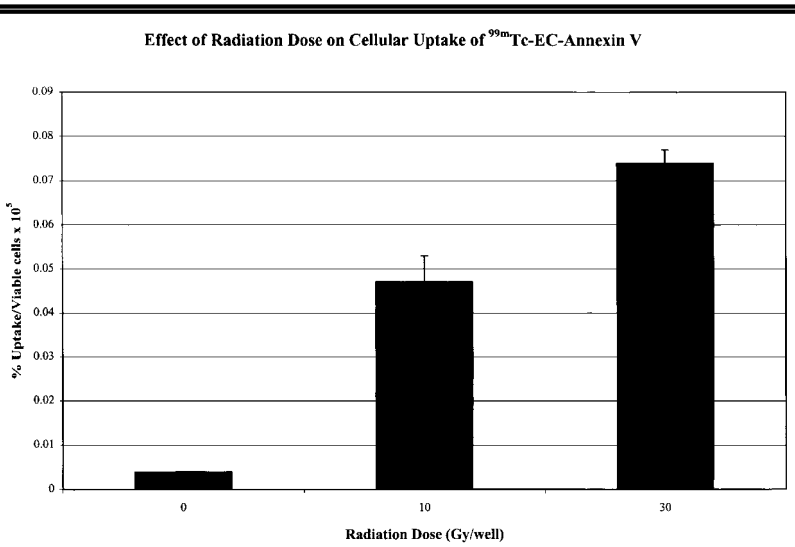

Figure 5. Breast tumor cells (RBA CRL-1747, breast cancer cell line, 2.5×10^5 cell/5 ml buffer/well) were irradiated with a Cs-137 external beam source (0–30 Gy/well). After three-day incubation, cell viability was determined by MTT assay. ^{99m}Tc-EC-annexin (10μCi/well, 7.5μg/well) was added to the cells. Unbound ^{99m}Tc-EC-annexin was removed by centrifugation and the total volume containing cells was transferred to a test tube to count the activity. Significantly increased uptake of ^{99m}Tc-EC-annexin V was observed in radiation-treated groups (10 and 30 Gy) compared to non-treated groups at 2 hrs incubation. Each data represents an average of three measurements, that were calculated as percentage of uptake per number of viable cells.

Table 1. Biodistribution of ^{99m}Tc-EC in Breast Tumor-Bearing Rats

	% of injected ^{99m}Tc-EC dose per organ or tissue			
	30 min	*1 h*	*2 h*	*4 h*
Blood	0.435 ± 0.029	0.273 ± 0.039	0.211 ± 0.001	0.149 ± 0.008
Lung	0.272 ± 0.019	0.187 ± 0.029	0.144 ± 0.002	0.120 ± 0.012
Liver	0.508 ± 0.062	0.367 ± 0.006	0.286 ± 0.073	0.234 ± 0.016
Stomach	0.136 ± 0.060	0.127 ± 0.106	0.037 ± 0.027	0.043 ± 0.014
Kidney	7.914 ± 0.896	8.991 ± 0.268	9.116 ± 0.053	7.834 ± 1.018
Thyroid	0.219 ± 0.036	0.229 ± 0.118	0.106 ± 0.003	0.083 ± 0.005
Muscle	0.060 ± 0.006	0.043 ± 0.002	0.028 ± 0.009	0.019 ± 0.001
Intestine	0.173 ± 0.029	0.787 ± 0.106	0.401 ± 0.093	0.103 ± 0.009
Urine	9.124 ± 0.808	11.045 ± 6.158	13.192 ± 4.505	8.693 ± 2.981
Tumor	0.342 ± 0.163	0.149 ± 0.020	0.115 ± 0.002	0.096 ± 0.005
Tumor/Blood	0.776 ± 0.322	0.544 ± 0.004	0.546 ± 0.010	0.649 ± 0.005
Tumor/Muscle	5.841 ± 3.253	3.414 ± 0.325	4.425 ± 1.397	5.093 ± 0.223
Tumor/Lung	1.256 ± 0.430	0.797 ± 0.022	0.797 ± 0.002	0.798 ± 0.007

Values shown represent the mean ± standard deviation of data from 3 animals.

that map the location and concentration of radionuclide-labeled radiotracers. Although CT and MRI provide considerable anatomic information about the location and the extent of tumors, these imaging modalities cannot adequately differentiate invasive lesions from edema, radiation necrosis, or gliosis.[47–51] PET and SPECT have been used to localize and characterize tumors by measuring functional and metabolic activities.

To characterize tumors, radiolabeled ligands, radiolabeled antibodies, and signal transduction agents have opened a new era and have undergone extensive preclinical development and evaluation.[52,53] The strategy of labeling biomolecules for molecular imaging has generated considerable interest, but focus must first be on the stability and efficient attachment of isotopes. Several ^{99m}Tc-labeling techniques have been reported, and they include N_4 (e.g. DOTA), N_3S (e.g., MAG-3), N_2S_2 (e.g., ECD), NS_3, S_4 (e.g.,

Table 2. Biodistribution of ^{99m}Tc-EC-Annexin V in Breast Tumor-Bearing Rats

	% of injected ^{99m}Tc-EC-Annexin V dose per organ or tissue		
	30 min	*2 h*	*4 h*
Blood	0.917 ± 0.037	0.379 ± 0.071	0.211 ± 0.007
Lung	0.537 ± 0.022	0.238 ± 0.035	0.152 ± 0.006
Liver	3.952 ± 0.310	3.062 ± 0.936	2.845 ± 0.047
Stomach	0.256 ± 0.028	0.616 ± 0.511	0.086 ± 0.007
Spleen	1.315 ± 0.048	3.659 ± 2.776	0.962 ± 0.075
Kidney	6.971 ± 0.974	4.907 ± 2.362	6.522 ± 0.303
Thyroid	0.465 ± 0.069	0.364 ± 0.221	0.126 ± 0.004
Muscle	0.092 ± 0.009	0.038 ± 0.011	0.020 ± 0.002
Intestine	0.202 ± 0.014	0.114 ± 0.022	0.080 ± 0.005
Tumor	0.429 ± 0.043	0.268 ± 0.064	0.173 ± 0.011
Tumor/Blood	0.466 ± 0.029	0.695 ± 0.033	0.818 ± 0.022
Tumor/Muscle	4.650 ± 0.021	7.363 ± 0.737	8.557 ± 0.622
Tumor/Lung	0.797 ± 0.050	1.101 ± 0.096	1.141 ± 0.086

Values shown represent the mean ± standard deviation of data from 3 animals.

Note: ^{99m}Tc-EC-annexin V is an apoptosis marker. Unlike ^{99m}Tc-EC (Table 1) and ^{99m}Tc-pertechnetate, tumor-to-tissue count density ratios increased as a function of time.

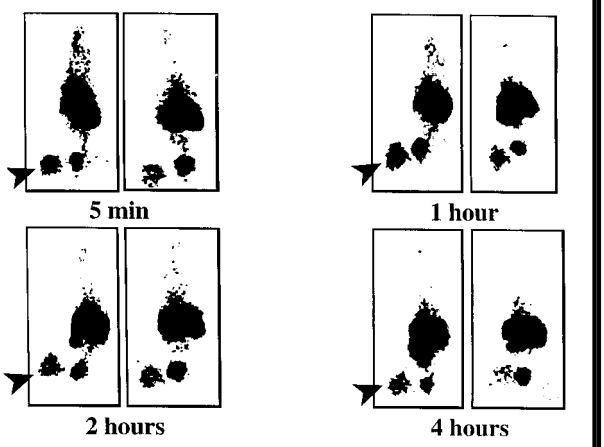

Figure 6. Planar images of breast tumor-bearing rats following administration of ^{99m}Tc-EC-annexin V (100 μCi/rat, iv.) showed that tumor uptake could be visualized from 5 min to 4 hrs on day 14 after inoculation of tumor cells.

sulfur colloid), DTPA, and HYNIC.[30–32,37,54–56] Among these chelators, the DTPA moiety does not chelate with ^{99m}Tc as stably as with ^{111}In.[56] The HYNIC technique requires two additional chemicals (tricine, triphenylphosphine) in order to form a Tc-99m complex, thus making it inconvenient to formulate in a kit form and costly. The nitrogen and sulfur combination has been shown to be a stable chelator for ^{99m}Tc. Bisaminoethanethiol tetradentate ligands, also called diaminodithiol compounds, are known to form very stable Tc(V)O-complexes on the basis of efficient binding of the oxotechnetium group to two thiolsulfur and two amine nitrogen atoms. ^{99m}Tc-ethylenedicysteine (^{99m}Tc-EC) is a successful example of N_2S_2 chelates. Using a standard coupling technique, ^{99m}Tc-EC-drug conjugates were then developed to characterize tumor tissues.[57,58] In vivo biodistribution and planar imaging studies in tumor-bearing rats given ^{99m}Tc-EC-annexin V demonstrated the pharmacokinetic distribution of the tracer and feasibility of using this molecular marker to image tumors. Tumor-to-tissue count density ratios were increased as a function of time suggesting that ^{99m}Tc-EC-annexin V is a tumor specific marker.

Apoptosis occurs during the treatment of cancer with chemotherapy and radiation. Apoptosis can be induced by antibiotics, radiation, Fas-mediated antibody, and anticancer drugs.[25,26,59–62] Apoptosis can occur early, therefore both tumor volume and tumor uptake of annexin need to be measured. Annexin V is known to bind to phosphatidylserine, which is overexpressed by tumor apoptotic cells. Assessment of apoptosis by annexin V could be useful to evaluate the efficacy of therapy and disease progression or regression. Decreased tumor volume, increased uptake of annexin at an early time, and later decreased uptake after treatment would reflect a positive treatment response.

The timing of apoptosis may have occurred at earlier time interval as evidenced by increased ROI ratios at 2 hrs on day 3 post-treatment. However, at day 18 (day 5 post-treatment), both apoptosis and necrosis may have occurred and that may account for tumor response. To demonstrate cellular distribution of ^{99m}Tc-EC-annexin V with and without paclitaxel or radiation treatment, microautoradiographic technique would provide detailed information on the distribution of ^{99m}Tc-EC-annexin V in a whole intact cell from the membrane to the nucleus.

In summary, a simple labeling method for

Table 3. Assessment of Paclitaxel Treatment Response Using ^{99m}Tc-EC-annexin V

	Tumor/Background ratios from ROI		
Imaging Time	*Pre-treatment (d14)*	*Post-treatment (d16)*	*Post-treatment (d18)*
5 min	2.64 ± 0.25	2.91 ± 0.25	2.81 ± 0.05
1 hour	4.03 ± 0.01	4.81 ± 0.11*	3.94 ± 0.14
2 hours	5.38 ± 0.04	5.74 ± 0.04*	4.75 ± 0.07*
4 hours	5.08 ± 0.06	5.83 ± 0.08*	4.90 ± 0.09
Tumor Volume (mm^3)	6260.5 ± 134.3	6817.5 ± 174.8	5904.3 ± 102.1

*$P < 0.05$ (compared to pre-treatment) (n = 3)
Tumor volume (mm^3) = [length × width × height]/2

preparation of high specific activity ^{99m}Tc-EC-annexin was developed. In vitro cell culture revealed that there was significantly increased cellular uptake of ^{99m}Tc-EC-annexin after irradiation or paclitaxel treatment. This increased uptake was likely due to the formation of apoptotic bodies as shown by Hoechst staining. In vivo imaging studies showed that there were transiently increased tumor/non-tumor ratios after paclitaxel treatment. In vitro and in vivo findings indicate that ^{99m}Tc-EC-annexin, a marker for apoptosis, may be useful in assessing the outcome of cancer treatment.

ACKNOWLEDGMENTS

The authors wish to thank Eloise Daigle for her secretarial support. This work was supported in part by the John S. Dunn Foundation and Pioneer Pharmaceutical Research Fund. The animal research was supported by M. D. Anderson Cancer Center (CORE) Grant NIH CA-16672.

REFERENCES

1. Ulsperger E, Karrer K. Tumor markers for the diagnosis, prognosis, treatment and follow-up of gynaecological tumors. *Bull Soc Sci Med Grand Duche Luxemb* 1989;126:33–43.
2. Jensen JL, Maclean GD, Suresh MR, et al. Possible utility of serum determinations of CA 125 and CA 27.29 in breast cancer management. *Int J Biol Markers.* 1991; 6:1–6.
3. Mehta TS, Raza S, Baum JK. Use of Doppler ultrasound in the evaluation of breast carcinoma. *Semin Ultrasound CT MR* 2000;21:297–307.
4. Avril N, Rose CA, Schelling M, et al. Breast imaging with positron emission tomography and fluorine-18 fluorodeoxyglucose: use and limitations. *J Clin Oncol.* 2000;18:3495–3502.
5. Tsugawa K, Noguchi M, Miwa K, et al. Dye- and gamma probe-guided sentinel lymph node biopsy in breast cancer patients: using patent blue dye and technetium-99m-labeled human serum albumin. *Breast Cancer* 2000;7(1):87–94.
6. Kasamaki S, Tsurumaru M, Kamano T, et al. A case of inflammatory breast cancer following augmentation mammoplasty with silicone gel implants. *Breast Cancer* 2000;7:71–4.
7. Mandelson MT, Oestreicher N, Porter PL, et al. Breast density as a predictor of mammographic detection: comparison of interval- and screen-detected cancers. *J Natl Cancer Inst* 2000;92(13):1081–7.
8. Park BW, Kim SI, Kim MH, et al. Clinical breast examination for screening of asymptomatic women: the importance of clinical breast examination for breast cancer detection. *Yonsei Med J* 2000;41:312–8.
9. Ando Y, Fukatsu H, Ishiguchi T, et al. Diagnostic utility of tumor vascularity on magnetic resonance imaging of the breast. *Magn Reson Imaging* 2000;18(7): 807–813.
10. Sutherland RL, Prall OW, Watts CK, et al. Estrogen and progestin regulation of cell cycle progression. *J Mammary Gland Biol Neoplasia* 1998;3:63–72.
11. Klaholz BP, Mitschler A, Moras D. Structural basis for isotype selectivity of the human retinoic acid nuclear receptor. *J Mol Biol* 2000;302:155–70.
12. Kurt RA, Urba WJ, Schoof DD. Isolation of genes overexpressed in freshly isolated breast cancer specimens. *Breast Cancer Res Treat* 2000;59(1):41–8.
13. Lin SY, Xia W, Wang JC, et al. Beta-catenin, a novel prognostic marker for breast cancer: its roles in cyclin D1 expression and cancer progression. *Proc Natl Acad Sci U S A* 2000;97(8):4262–6.
14. Ozer E, Sis B, Ozen E, et al. BRCA1, C-erbB-2, and H-ras gene expressions in young women with breast cancer. An immunohistochemical study. *Appl Immunohistochem Molecul Morphol* 2000;8:12–8.
15. Ilgan S, Yang DJ, Higuchi T, et al. Imaging tumor folate receptors using ^{111}In-DTPA-methotrexate. *Cancer Biother Radiopharm* 1998;13:177–84.
16. Stempien-Otero A, Karsan A, Cornejo CJ, et al. Mechanisms of hypoxia-induced endothelial cell death. Role of p53 in apoptosis. *Biol Chem* 1999;274:8039–45.
17. Martin SJ, Reutelingsperger CP, McGahon AJ, Rader JA, van Schie RC, LaFace DM, Green DR. Early redistribution of plasma membrane phosphatidylserine is a general feature of apoptosis regardless of the initiating stimulus: inhibition by overexpression of Bcl-2 and Abl. *J Exp Med* 1995;182(5):1545–56.
18. Saikumar P, Dong Z, Weinberg JM, et al. Mechanisms of cell death in hypoxia/reoxygenation injury. *Oncogene* 1998;17:3341–9.
19. Yun JK, McCormick TS, Villabona C, et al. Inflammatory mediators are perpetuated in macrophages resistant to apoptosis induced by hypoxia. *Proc Natl Acad Sci U S A* 1997;94:13903–8.
20. Dive C, Gregory CD, Phipps DJ, et al. Analysis and discrimination of necrosis and apoptosis (programmed cell death) by multiparameter flow cytometry. *Biochim Biophys Acta* 1992;1133:275–85.
21. Narula J, Hajjar RJ, Dec GW. Apoptosis in the failing heart. *Cardiol Clin* 1998;16:691–710.
22. Bossenmeyer-Pourie C, Koziel V, Daval J. CPP32/CASPASE-3-like proteases in hypoxia-induced apoptosis in developing brain neurons. *Brain Res Mol Brain Res* 1999;71:225–37.
23. Banasiak KJ, Cronin T, Haddad GG. bcl-2 prolongs neuronal survival during hypoxia-induced apoptosis. *Brain Res Mol Brain Res* 1999;72:214–25.
24. Bronckers AL, Goei SW, Dumont E, Lyaruu DM, Woltgens JH, van Heerde WL, Reutelingsperger CP, van den Eijnde SM. In situ detection of apoptosis in dental and periodontal tissues of the adult mouse us-

ing annexin-V-biotin. *Histochem Cell Biol* 2000; 113(4):293–301.
25. Tait JF, Smith C. Site-specific mutagenesis of annexin V: role of residues from Arg- 200 to Lys-207 in phospholipid binding. *Arch Biochem Biophys* 1991;288: 141–144.
26. Blankenberg FG, Katsikis PD, Tait JF, et al. Imaging of apoptosis (programmed cell death) with ^{99m}Tc-annexin. *J Nucl Med* 1999;40:184–191.
27. Czarnota GJ, Kolios MC, Abraham J, et al. Ultrasound imaging of apoptosis: high-resolution non-invasive monitoring of programmed cell death in vitro, in situ and in vivo. *Br J Cancer* 1999;81:520–7.
28. Zucker RM, Hunter ES 3rd, Rogers JM. Apoptosis and morphology in mouse embryos by confocal laser scanning microscopy. *Methods* 1999;18:473–80.
29. Ernst JD, Yang L, Rosales JL, Broaddus VC. Preparation and characterization of an endogenously fluorescent annexin for detection of apoptotic cells. *Anal Biochem* 1998;260(1):18–23.
30. Ogura Y, Krams SM, Martinez OM, et al. Radiolabeled annexin V imaging: diagnosis of allograft rejection in an experimental rodent model of liver transplantation. *Radiology* 2000;214(3):795–800.
31. Ohtsuki K, Akashi K, Aoka Y, Blankenberg FG, Kopiwoda S, Tait JF, Strauss HW. Technetium-99m HYNIC-annexin V: a potential radiopharmaceutical for the in-vivo detection of apoptosis *Eur J Nucl Med* 1999;26(10):1251–8.
32. Vriens PW, Blankenberg FG, Stoot JH, et al. The use of technetium ^{99m}Tc annexin V for in vivo imaging of apoptosis during cardiac allograft rejection. *J Thorac Cardiovasc Surg* 1998;116:844–53.
33. Davison A, Jones AG, Orvig C, Sohn M. A new class of oxotechnetium(+5) chelate complexes containing a $TcON_2S_2$ Core. *Inorg Chem* 1980;20:1629–1632.
34. Verbruggen AM, Nosco DL, Van Nerom CG, et al. ^{99m}Tc-L,L-ethylenedicysteine: A renal imaging agent. Labelling and evaluation in animals. *J Nucl Med* 1992; 33:551–557.
35. Van Nerom CG, Bormans GM, De Roo MJ, et al. First experience in healthy volunteers with ^{99m}Tc-L,L-ethylenedicysteine, a new renal imaging agent. *Eur J Nucl Med* 1993;20:738–746.
36. Surma MJ, Wiewiora J, Liniecki J. Usefulness of ^{99m}Tc-N,N-ethylene-1-dicysteine complex for dynamic kidney investigations. *Nucl Med Comm* 1994;15:628–635.
37. Verbruggen A, Nosco D, Van Nerom C, et al. Evaluation of ^{99m}Tc-L,L-ethylenedicysteine as a potential alternate to ^{99m}Tc-MAG3. *Eur J Nucl Med* 1990;16:429.
38. Van Nerom C, Bormans G, Bauwens J, et al. Comparative evaluation of ^{99m}Tc-L,L-ethylenedicysteine and ^{99m}Tc-MAG3 in volunteers. *Eur J Nucl Med* 1990; 16:417.
39. Jamar F, Stoffel M, Van Nerom C, et al. Clinical evaluation of ^{99m}Tc-L,L-ethylenedicysteine, a new renal tracer, in transplanted patients. *J Nucl Med* 1993;34: 129P.
40. Jamar F, Van Nerom C, Verbruggen A, et al. Clearance of the new tubular agent ^{99m}Tc-L,L-ethylenedicysteine: Estimation by a simplified method. *J Nucl Med* 1993; 34:129P.
41. Ratner S, Clarke HT. The action of formaldehyde upon cysteine. *J Am Chem Soc* 1937;59:200–206.
42. Blondeau P, Berse C, Gravel D. Dimerization of an intermediate during the sodium in liquid ammonia reduction of L-thiazolidine-4-carboxylic acid. *Can J Chem* 1967;45:49–52.
43. Yang DJ, Tewson T, Tansey W, et al. Halogenated analogs of tamoxifen: synthesis, receptor assay and inhibition of MCF7 cells. *J Pharm Sci* 1992;81:622–625.
44. Maciorowski Z, Delic J, Padoy E, et al. Comparative analysis of apoptosis measured by Hoechst and flow cytometry in non-Hodgkin's lymphomas. *Cytometry* 1998;32:44–50.
45. Stodilka RZ, Kemp BJ, Prato FS, et al. Scatter and attenuation correction for brain SPECT using attenuation distributions inferred from a head atlas. *J Nucl Med* 2000;41:1569–78.
46. Kao CH, ChangLai SP, Chieng PU, et al. Technetium-99m methoxyisobutylisonitrile chest imaging of small cell lung carcinoma: relation to patient prognosis and chemotherapy response—a preliminary report. *Cancer* 1998;83:64–8.
47. Imai Y, Murakami T, Yoshida S, et al. Superparamagnetic iron oxide-enhanced magnetic resonance images of hepatocellular carcinoma: correlation with histological grading. *Hepatology* 2000;32:205–12.
48. De Schepper AM, De Beuckeleer L, Vandevenne J, et al. Magnetic resonance imaging of soft tissue tumors. *Eur Radiol* 2000;10:213–23.
49. Nowak B, Di Martino E, Janicke S, et al. Diagnostic evaluation of malignant head and neck cancer by F-18-FDG PET compared to CT/MRI. *Nuklearmedizin* 1999;38:312–8.
50. Kihlstrom L, Karlsson B. Imaging changes after radiosurgery for vascular malformations, functional targets, and tumors. *Neurosurg Clin N Am* 1999;10:167–80.
51. Barker FG, Chang SM, Valk PE, et al. 18-Fluorodeoxyglucose uptake and survival of patients with suspected recurrent malignant glioma. *Cancer* 1997;79: 115–26.
52. Brock CS, Meikle SR, Price P. Does ^{18}F-fluorodeoxyglucose metabolic imaging of tumors benefit oncology? *Eur J Nucl Med* 1997;24:691–705.
53. Goldsmith SJ. Receptor imaging: Competitive or complementary to antibody imaging. *Sem Nucl Med* 1997; 27:85–93.
54. Canet EP, Casali C, Desenfant A, An MY, Corot C, Obadia JF, Revel D, Janier MF. Kinetic characterization of CMD-A2-Gd-DOTA as an intravascular contrast agent for myocardial perfusion measurement with MRI. *Magn Reson Med* 2000;43(3):403–9.
55. Laissy JP, Faraggi M, Lebtahi R, Soyer P, Brillet G, Mery JP, Menu Y, Le Guludec D. Functional evaluation of normal and ischemic kidney by means of gadolinium-DOTA enhanced TurboFLASH MR imaging: a preliminary comparison with 99Tc-MAG3 dy-

namic scintigraphy. *Magn Reson Imaging* 1994;12(3): 413–9.
56. Mathias CJ, Hubers D, Trump DP, et al. Synthesis of ^{99m}Tc-DTPA-folate and preliminary evaluation as a folate-receptor-targeted radiopharmaceutical *J Nucl Med* 1997;38:87P (Abstract).
57. Ilgan, S, Yang, DJ, Higuchi, et al. ^{99m} Tc-Ethylenedicysteine-Folate: A new tumor imaging agent. Synthesis, labeling and evaluation in animals. *Cancer Biotherapy and Radiopharm* 1998;13:427–435.
58. Zareneyrizi F, Yang DJ, Oh C-S, et al. Synthesis of ^{99m}Tc-ethylenedicysteine-colchicinefor evaluation of antiangiogenic efffect. *Anti-Cancer Drugs* 1999;10:685–692.
59. Lennon SV, Martin SJ, Cotter TG. Dose-dependent induction of apoptosis in human tumor cell lines by widely diverging stimuli. *Cell Prolif* 1991;24:203–214.
60. Abrams MJ, Juweid M, Tenkate CI. ^{99m}Tc-human polyclonal IgG radiolabeled via the hydrazino nicotinamide derivative for imaging focal sites of infection in rats. *J Nucl Med* 1990;31:2022–2028.
61. Blankenberg FG, Katsikis PD, Tait JF, et al. In vivo detection and imaging of phosphatidylserine expression during programmed cell death. *Proc Natl Acad Sci USA* 1998;95:6349–6354.
62. Blankenberg F, Narula J, Strauss HW. In vivo detection of apoptotic cell death: a necessary measurement for evaluating therapy for myocarditis, ischemia, and heart failure. *J Nucl Cardiol* 1999;6:531–9.